TABLE II: Calculated and Observed[a] pK Values for the Na^+, Ca^{2+}, and Mg^{2+} Aquo Cations[a]

ion	pK^{calc}	pK^{obs}
(H_2O)	15.7	15.7
Na^+	14.5	14.6-14.8
Ca^{2+}	13.0	12.6
Mg^{2+} (old)	6.4	11.4
Mg^{2+} (new)	11.5	11.4

[a] Convergence errors in calculated numbers are ±0.6-0.7 pK units.

function (RDF) peak for Mg^{2+} is 2.10 Å while the calculated one reported in ref 3 is 2.00 Å. This seemingly small difference will not have a great impact on the energetics of interactions with moderately polar ligands. However, it appears that the interaction of the metal with the fully charged OH^- ion becomes significantly overestimated due to the small Mg^{2+} radius. The conclusion to be drawn from this result is that great care must be given to both the RDF and ΔG^{hydr} when the ion parameters are calibrated.

We therefore made an effort to derive a new Mg^{2+} potential in order to be able to reproduce the relvant RDF peak more accurately while still maintaining the correct hydration energy. This requires that both the repulsive and attractive LJ parameters be made considerably larger since one essentially has to move some of the metal-ligand attraction from electrostatic to van der Waals energy. The final parameters arrived at in recalibrating Mg^{2+} were $(A_{Mg}, B_{Mg}) = (96.0, 32.0)$. The resulting ion-water oxygen RDF peak for this potential is found at 2.08 Å while the calculated value of the hydration energy is $\Delta G^{hydr}_{calc} = -454.0 \pm 2.0$ kcal/mol ($\Delta G^{hydr}_{obs} = -455.5$ kcal/mol). The calibration above was carried out in exactly the same way as in ref 3.

The effect of the new Mg^{2+} model on the energetics of the PT reaction is also shown in Figure 3 (lower curve). The stabilization of the ion-pair configuration now becomes less pronounced than was the case with the previous Mg^{2+} parameters. The new Mg^{2+} potential gives a reaction free energy of $\Delta G°_{calc} = 15.6$ kcal/mol which is in much better agreement with the experimental result than for the old model. The average Mg^{2+}-OH^- distance is now 2.04 Å, as compared to 1.91 Å previously, which is rather close to the sum of the Pauling radii for the two ions (2.05 Å).

The results of the present calculations of the metal ion catalyzed PT reaction (eq 1) are summarized in Table II in terms of pK values for the corresponding aquo cations. As an additional check we also evaluated the pK shifts by the thermodynamic cycle corresponding to $H_2O(aq) \rightarrow OH^-(aq)$, with and without metals present, and this approach yielded essentially identical results. Apart from the deficiency of the original Mg^{2+} parameters, the results are thus quite encouraging in our opinion. That is, the current ion potential functions have been found to fulfill the three crucial tests of reproducing the observed ΔG^{hydro}'s, ion-oxygen RDF peaks and the acidity of the corresponding aquo cations. Moreover, we recall the study of alkali-metal ion complexation with valinomycin[5] which demonstrated that the selectivity pattern of this molecule could be quantitatively reproduced with the current potentials. In the context of ion-protein interactions, it might also be worth mentioning two earlier studies of the energetics of ion solvation in the gramicidin A transmembrane channel[16] and of the staphylococcal nuclease catalyzed reaction.[7] Although the ion parameters used in these studies are not identical with the present ones, they are quite similar and the studies of refs 16 and 7 provide the first examples of (FEP/MD) calculations of absolute binding constants for an ion-binding protein site and of the catalytic effect of metal ions in enzymes. The picture emerging from the work reported in refs 5, 7, and 16, as well as other calculations of relative ion binding constants for small molecules[17] and the present study, indicates that we are actually reaching a stage where interactions with ions in rather complex molecular systems can be quantitatively modeled by computational chemistry techniques.

Acknowledgment. This work was supported by a grant from the Swedish Natural Science Research Council.

(15) Magini, M. In *Ions and Molecules in Solution*; Tanaka, N., Ohtaki, H., Tamamushi, R., Eds.; Elsevier: Amsterdam, 1983; p 97.

(16) Åqvist, J.; Warshel, A. *Comm. Mol. Cell. Biophys.* **1989**, *6*, 91.

(17) (a) Lybrand, T. P.; McCammon, J. A.; Wipff, G. *Proc. Natl. Acad. Sci. U.S.A.* **1986**, *83*, 833. (b) Grootenhuis, P. D. J.; Kollman, P. A. *J. Am. Chem. Soc.* **1989**, *111*, 2152.

(18) Drawn with the program MOLSCRIPT. Kraulis, P. J., submitted for publication.

Direct Visualization of Monolayers at the Air-Water Interface by Brewster Angle Microscopy

Dirk Hönig* and Dietmar Möbius

Max-Planck-Institut für biophysikalische Chemie, Postfach 2841, D-3400 Göttingen, Germany

(Received: February 26, 1991)

No light is reflected from the air-water interface under Brewster angle incidence if p-polarized light is used. With constant angle of incidence, the formation of a monolayer on the water surface modifies the Brewster angle condition, and light reflection is observed. Reflectivity-area isotherms of arachidic acid monolayers on pure water and on aqueous solutions of different pH have been measured. Areas of different brightness due to different molecular density and/or refractive index in the monolayer have been recorded with a video system as micrographic pictures. This Brewster angle microscopy enables us also to detect monolayer inhomogeneities and the reversible formation of solid-phase domains upon compression of monolayers of DMPE.

Reflection spectroscopy under normal and oblique incidence of light is an extremely useful technique for the investigation of molecular organization and of chemical reactions of dye monolayers at the air-water interface.[1-4] Light reflection under normal incidence has been measured in order to determine the thickness of nonabsorbing monolayers on water.[5] In all these investigations the reflectivity of the air-water or air-solution interface in the absence of the monolayer was a background signal to the change in reflectivity.

(1) Grüniger, H.; Möbius, D.; Meyer, H. *J. Chem. Phys.* **1983**, *79*, 3701.

(2) Orrit, M.; Möbius, D.; Lehmann, U.; Meyer, H. *J. Chem. Phys.* **1986**, *85*, 4966.

(3) Loschek, R.; Möbius, D. *Chem. Phys. Lett.* **1988**, *151*, 176.

(4) Lehmann, U. *Thin Solid Films* **1988**, *160*, 257.

(5) Dhathathreyan, A.; Baumann, U.; Müller, A.; Möbius, D. *Biochim. Biophys. Acta* **1988**, *944*, 265.

0022-3654/91/2095-4590$02.50/0

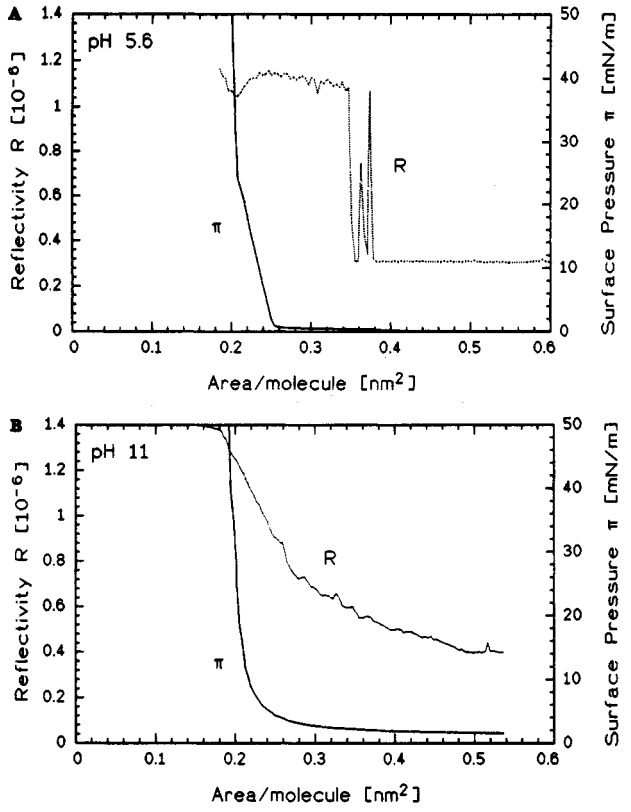

Figure 1. Surface pressure (π/A) and reflectivity (R/A) area isotherms of monolayers of arachidic acid on pure water (a) and on water with pH = 11, adjusted by addition of NaOH (b). T = 20.5 °C.

This background can be nearly entirely eliminated by using p-polarized light under Brewster angle incidence. The contrast arises from the formation of a thin layer with a refractive index different from that of the subphase. At solid surfaces, this experimental situation has been used to study the adsorption of proteins at a silica–solution interface[6] or for monitoring epitaxial growth of GaAs by metalloorganic chemical vapor deposition.[7,8] To our knowledge, this technique has not yet been used for the investigation of monolayers at the air–water interface.

Reflection/Area Isotherms. The reflectivity $R = I/I_0$ (I, reflected intensity, I_0, incident intensity) of the water surface at the Brewster angle under p-polarization was recorded simultaneously with the surface pressure π as a function of the area per molecule. Therefore, the reflected light of a laser diode (power <1 mW, wavelength 670 nm, light spot diameter ≈1 mm) in combination with a polarizer was detected with a photomultiplier. The angles of incidence and observation were fixed to the Brewster angle for the pure water subphase. Further experimental details will be described elsewhere. Figure 1 shows the π/A and R/A isotherms of arachidic acid (AA) on pure water (A) and on water of pH = 11, adjusted by addition of NaOH (B). Both types of isotherms obviously depend on the pH of the subphase. On pure water (Figure 1A), the reflection isotherm is constant in the beginning of the compression, i.e., at large values of A. The reflectivity measured here is the same as that found for pure water. The peaks occurring at $A \approx 0.34$ nm²/molecule are due to domains of solid monolayer passing the illuminated spot. The abrupt increase upon compression at 0.32 nm²/molecule, clearly before the surface pressure rises, is observed when the front of the monolayer material collected in front of the moving barrier reaches the light spot.

The situation is completely different for subphase pH = 11 (Figure 1B). An increased reflectivity with respect to the bare subphase is observed immediately after spreading of the AA monolayer, and the R/A isotherm shows a continuous rise upon compression. We attribute this behavior to a homogeneous distribution of the monolayer material due to the repulsion of the ionized head groups. It is interesting with respect to head-group ionization that a behavior like that shown in Figure 1A is also observed for a subphase pH = 9.3 in contrast to the general assumption of complete COOH group ionization in AA monolayers at such a pH.

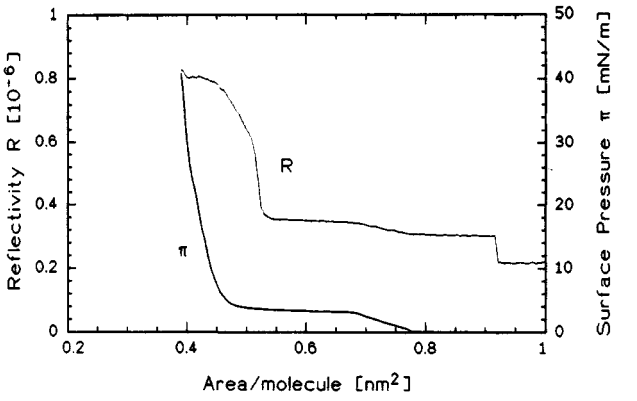

Figure 2. Surface pressure (π/A) and reflectivity (R/A) area isotherms of DMPE (dimyristoylphosphatidylethanolamine) on pure water. T = 20.5 °C.

The pronounced phase transition in monolayers of DMPE (dimyristoylphosphatidylethanolamine) on water has been investigated in much detail by measurement of π/A and surface potential/A isotherms[9] as well as by fluorescence microscopy.[10] Figure 2 shows the π/A and R/A isotherm of DMPE on pure water at 20.5 °C. At A = 0.92 nm²/molecule the reflectivity increases abruptly from the water value to that of the front of liquid monolayer. A modest increase of R is observed upon compression when the surface pressure starts to rise, and a plateau of the R/A isotherm is observed in coincidence with that of the π/A isotherm. This plateau is difficult to interpret since either the thickness or the refractive index of the monolayer or both should change in this section of the isotherm (between 0.68 and 0.53 nm²/molecule) which would give rise to a change in R. This part of the π/A isotherm has been attributed to a phase transition from LE (liquid expanded) to LC (liquid condensed).[10] The reflectivity increases sharply at the end of the nearly horizontal part of the π/A isotherm (at 0.53 nm²/molecule) similar to what is observed for the surface potential.[8] This sudden rise indicates the appearance of the solid phase with a refractive index different from that of the liquid monolayer phase. The reflectivity becomes constant at an area of 0.43 nm²/molecule.

Brewster Angle Microscopy. Due to a different distribution of a fluorescent probe in solid domains as compared to the liquid monolayer phase, the solid domains can be detected. The influence of the fluorescent probe on formation and growth of solid domains, however, is not known. It is particularly difficult to determine the end of the phase transition upon compression, since the probe is enriched in the fluid phase. The direct observation of domains in the absence of any probe by light reflection eliminates such problems. For Brewster angle microscopy (BAM), the laser diode used for the reflectivity measurements was replaced by a HeNe laser (power 8 mW, spot diameter ≈1 mm) for higher light intensity. On the detection side, the photomultiplier tube was removed and the reflecting spot at the air–water interface was imaged at 4× magnification, using a lens onto the chip of a conventional CCD video camera. According to the spatial resolution of the CCD, chip objects of about 3-μm diameter can be visualized. Details will be published elsewhere.

There are two main limitations for the image quality in this setup. One is the interference pattern caused by the optical components of the system and the coherent laser light. By

(6) Schaaf, P.; Dejardin, P.; Schmitt, A. *Langmuir* **1987**, *3*, 1131.
(7) Makimoto, T.; Yamauchi, Y.; Kobayashi, N.; Horikoshi, Y. *Jpn. J. Appl. Phys.* **1990**, *29*, L207.
(8) Makimoto, T.; Yamauchi, Y.; Kobayashi, N.; Horikoshi, Y. *Jpn. J. Appl. Phys.* **1990**, *29*, L645.
(9) Miller, A.; Helm, C. A.; Möhwald, H. *J. Phys. (Paris)* **1987**, *48*, 693.
(10) Möhwald, H.; Kenn, R. M.; Degenhardt, D.; Kjaer, K.; Als-Nielsen, J. *Physica A* **1990**, *168*, 127.

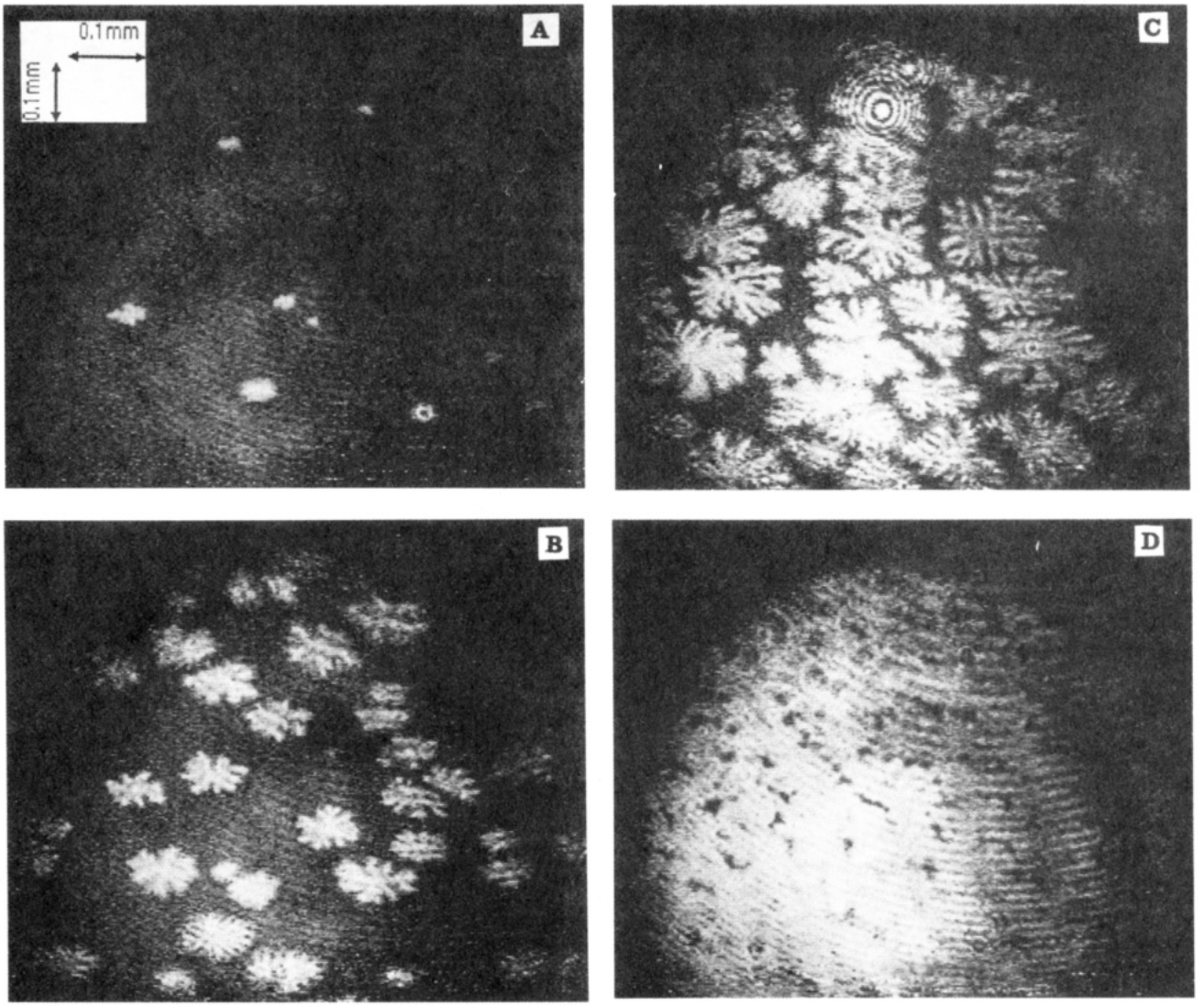

Figure 3. Brewster angle microscopy of a monolayer of DMPE on pure water; T = 18.5 °C. Video records of p-polarized light reflected under the Brewster angle for the pure water surface: formation of solid domains upon compression in the phase transition region at 0.52 ± 0.01 nm²/molecule (A); growth of the solid domains with characteristic shape upon further compression (B, C); determination of the end of the phase transition at 0.41 ± 0.01 nm²/molecule: disappearance of the dark area (D).

watching the video display during compression of the monolayer, one can clearly discriminate this pattern from the signal produced by the monolayer. This is more difficult when looking at still pictures or a photograph of the display. Another limitation of the image quality is due to the angle between the planes of the monolayer and the CCD chip with limited depth of field in focusing the image. It should be possible to overcome these limitations in future by the use of a digital image processing system.

A set of pictures recorded with the video camera upon compression of a monolayer of DMPE on pure water at 18.5 °C is shown in Figure 3A–D. The reversible formation of small solid domains at $A = 0.52 \pm 0.01$ nm²/molecule is clearly seen in Figure 3A as bright spots in a relatively dark area. Repeated compression and decompression allowed us to determine this area quite precisely. This area coincides quite well with the sudden rise (at 18.5 °C) in the R/A isotherm upon compression.

Upon further compression, the growth of the solid domains with a shape known from fluorescence microscopy is clearly observed with BAM (Figure 3B,C). The end point of the phase transition is reached when no dark area is left. Figure 3D shows the situation very close to the end which has been determined by repeated compression and decompression to occur at $A = 0.41 \pm 0.01$ nm²/molecule. The areas observed by BAM differ from those determined by fluorescence microscopy.[10]

In conclusion, it can be stated that Brewster angle reflectometry is a very sensitive optical technique that provides new information on monolayer organization. By Brewster angle microscopy a transparent monolayer can be visualized without addition of fluorescent probes. Monolayer organization can be monitored quite easily, and domains of different refracting properties are discriminated. Therefore, the new technique is an extremely valuable tool for monolayer characterization.

Acknowledgment. This work was financially supported by the Bundesministerium für Forschung und Technologie (O3 M4008 D).